Published in final edited form as:
Exp Eye Res. 2010 January ; 90(1): 155–167. doi:10.1016/j.exer.2009.10.004.

Low Nitric Oxide Synthases (NOS) in Eyes with Age-related Macular Degeneration (AMD)

Imran A. Bhutto, **Takayuki Baba**, **Carol Merges**, **D. Scott McLeod**, and **Gerard A. Lutty***
Department of Ophthalmology, The Wilmer Ophthalmological Institute, Johns Hopkins University School of Medicine, Baltimore, Maryland

Abstract

Nitric oxide (NO) production by vascular endothelium is important in regulation of blood flow. Reduced production of NO can adversely affect blood flow and other vascular functions. We investigated the expression of three nitric oxide synthase (NOS) isoforms in retina and choroid of aged human eyes and eyes with AMD.

Alkaline phosphatase immunohistochemistry was performed using antibodies against inducible (iNOS), neuronal (nNOS), and endothelial (eNOS) NOSs on cryopreserved sections from aged control donor eyes (n= 13) and eyes with AMD (n= 22). CD34 antibody was used as an endothelial cell (EC) marker. Three independent masked observers scored the intensity of the immunohistochemical reaction product. Mean scores from the aged control and AMD eyes were statistically compared.

In aged control retinas, nNOS was in ganglion cells (RGCs) and neurons of both nuclear layers. In choroid, perivascular nerve fibers and retinal pigment epithelial (RPE) cells were $nNOS^+$. eNOS and iNOS were confined to the retinal and choroidal vascular ECs. Some cells presumably melanocytes or dendritic cells in choroid were also $eNOS^+$. In AMD eyes, nNOS was significantly lower in RGCs, neurons, retinal vessels and RPE ($p \leq 0.05$) compared to the aged control eyes. iNOS and eNOS showed no significant differences between aged control and AMD eyes except that there was significantly less eNOS in choroidal arteries ($p=0.006$) and choroidal cells ($p=0.03$) of AMD eyes.

Although NO was not measured directly, these findings suggest that there is less NO produced in AMD eyes. The decrease in retinal nNOS in AMD eyes is probably related to neuronal degeneration. The decrease in nNOS and eNOS in AMD choroid could be associated with vasoconstriction and hemodynamic changes.

Keywords

age-related macular degeneration; nitric oxide synthases; retinal pigment epithelium; retinal endothelial cells; choriocapillaris; neurons

*Corresponding author Gerard A. Lutty, PhD G. Edward and G. Britton Durell Professor of Ophthalmology, Wilmer Ophthalmological Institute, M041 Smith Building, Johns Hopkins Hospital, 400 North Broadway, Baltimore, MD 21287-9115, USA. Tel: +1 410 955 6750; fax: +1 410 955 3447; galutty@jhmi.edu.

1. Introduction

Nitric oxide (NO) is an important signaling molecule that acts in many tissues to regulate a diverse range of physiological and cellular processes including neurotransmission, immune defense, the regulation of cell death (apoptosis), and cell motility. NO is a small, short-lived molecule, enzymatically synthesized from L-arginine by several isoforms of NO synthases (NOSs) (Alderton et al., 2001). Oxygen and nicotinamide adenine dinucleotide phosphate (NADPH) are necessary co-factors. The isoforms of NOS are divided into inducible NOS (iNOS) and constitutive NOS (cNOS) based on their nondependence and dependence, respectively, upon intracellular calcium/calmodulin for activity. cNOS is further classified as neuronal NOS (nNOS), the predominant isoform expressed in neurons, and endothelial NOS (eNOS), the predominant isoform in vascular endothelial cells. Once NO is formed by eNOS, it plays an important role in numerous vascular physiological processes, including regulation of blood pressure and blood flow, platelet aggregation, and leukocyte adhesion (Moncada et al., 1991; Palmer et al., 1987).

Choroidal blood flow is regulated by NO derived from the endothelial cells (eNOS) and perivascular nitrergic neurons (nNOS). Traditionally, eNOS, which is primarily a plasma membrane-bound protein (Griffith and Stuehr, 1995), generates NO in blood vessels and is involved with regulating vascular function. In recent years, a role of nNOS-generated NO in vascular function has been demonstrated (Boulanger et al., 1998; Ichihara et al., 1998; Toda and Okamura, 2003). Kashiwagi et al. (Kashiwagi et al., 2002) reported that nNOS-containing nerve fibers, which innervate arterioles and nerve terminals, are the major sources of arteriolar NO. Other studies have reported nNOS presence in perivascular nerve fibers (Nozaki et al., 1993). The choroid is known to receive abundant autonomic innervation. Both sympathetic and parasympathetic nerves have been found in the choroid (Cioffi GA et al., 2002; Lutjen-Drecoll, 2006; Ruskell, 1971). The sympathetic system was believed to govern the neural regulation of the choroidal blood flow and to prevent excessive blood flow by vasoconstriction. However, more recent findings have led to another concept on the control of choroidal blood flow and suggested that the parasympathetic (probably nitrergic) vasodilator nerves contribute significantly to the neural regulation of the choroidal blood flow (Flügel et al., 1994; Yamamoto et al., 1993).

The choroidal circulation provides nutrients to the photoreceptors and removes waste products from the retinal pigment epithelium (RPE). An abnormal choroidal blood supply may disrupt normal retinal function and lead to visual deterioration. Abnormalities of the choroidal circulation have been hypothesized to contribute to the development of age-related macular degeneration (AMD) (Grunwald et al., 1998a). We have previously observed severe loss of choriocapillaris (CC) and CC vasoconstriction in postmortem eyes of geographic atrophy (GA) subjects (McLeod et al., 2009; McLeod et al., 2002). However, there have been only a few studies to characterize the NOS isoforms in the choroid (Geyer et al., 1997). Therefore, the purpose of this study was to examine the immunolocalization of NOSs in human aged control donor eyes and to determine if the level and localization of NOS isoforms was altered in eyes with AMD. We focused on macular region because AMD most profoundly affects the submacular portion of the choroid. To our knowledge, this is the first study of the distribution of all three NOS isoforms in AMD eyes.

2. Materials and methods

2.1. Donor eyes

Human donor eyes were obtained with the help of Janet Sunness, M.D., and Carol Applegate (Greater Baltimore Medical Center, Baltimore, Maryland), and from certified eye banks through the National Disease Research Interchange (NDRI; Philadelphia, PA). Thirteen eyes

from aged human donors (mean age, 79.0±4.8 [SD] years) with no hard drusen and no other macular disease were classified as aged controls; 22 eyes from donors with clinically diagnosed with AMD (mean age, 82.5±9.9 [SD] years) were studied. Diagnosis of AMD was made by reviewing ocular medical history (if available), the eye bank sheets, and the postmortem gross examination of the posterior eyecup. They were classified according to the severity of disease: early AMD (n=12; soft indistinct drusen with or without pigmentary changes, or soft distinct drusen with pigmentary changes) or late (end-stage) AMD. The latter was sub-classified into geographic atrophy (n=6) or neovascular macular degeneration (n=4). Donors were all Caucasian. Table 1 shows the characteristics of each human donor subject used in this study. This study adhered to the tenets of the Declaration of Helsinki regarding research involving human tissue and was approved by the Johns Hopkins Medicine Institutional Review Board.

2.2. Tissue Preparation and Sectioning

The anterior segment of each eye was removed after a circumferential incision, approximately 5 mm from the limbus. A dissecting microscope (Stemi 2000; Carl Zeiss, Inc., Thornwood, NY) with a mounted digital camera (Q-imaging, Vancouver, BC) was used for gross examination of the posterior eyecup and to capture digital images. Images were imported directly into Adobe Photoshop (version 6.0; Adobe Systems Inc., San Jose, CA) on a PowerMac G3 (Apple Computer, Cupertino, CA). After examination and imaging, the posterior eyecups were fixed in 2% paraformaldehyde in 0.1 M sodium phosphate buffer (pH7.4) with 5% sucrose at room temperature for 1 hour. The tissue was cut into calottes of the vitreous–retina–choroid complex and cryopreserved with increasing concentrations of sucrose as previously described (Lutty et al., 1993). Serial 8-um thick cryosections were cut from the disc/macular blocks (extending from nasal peripapillary to two disc diameters temporal to macula), collected in duplicate on glass slides coated with Vectabond (Vector, Burlingame, CA), dried, and stored at −80°C.

2.3. Alkaline Phosphatase Immunohistochemistry and Histopathology

Streptavidin alkaline phosphatase (APase) immunohistochemistry was performed on cryosections for the localization of iNOS, nNOS, and eNOS using a nitroblue tetrazolium development system as previously described (Bhutto et al., 2004). Primary antibodies to NOSs included mouse anti-iNOS/NOS type II (dilution, 1:100; cat#610431; BD Biosciences, San Jose, CA), mouse anti-nNOS/NOS type I (dilution, 1:500; cat#610308; BD Biosciences, San Jose, CA), and rabbit polyclonal anti-eNOS (dilution, 1:500; cat#905–386; Assay Designs, Ann Arbor, MI). Mouse anti-human CD34 (dilution, 1:800; cat#SIG-3326–1000; Covance, Emeryville, CA) was used on adjacent sections to label blood vessels. As a negative control, the primary antibodies were omitted or a non-immune IgG was used at the same protein concentration as the primary antibody.

Melanin pigment in RPE and choroidal melanocytes was bleached as described previously (Bhutto et al., 2004). Three independent masked observers scored the relative intensity of the immunoreactivity for each antibody in retinal and choroidal structures using a previously described 7-point grading system (McLeod et al., 1995; Page et al., 1992). Immunoreactivity for NOS isoforms was not uniform but rather heterogenous, so the graders scored a particular structure throughout the whole tissue section.

Histopathology was evaluated on sections of the macula that were stained with the periodic acid Schiff's (PAS) and hematoxylin staining. In brief, the sections were treated in absolute methanol for 5 minutes, air dried, and placed into freshly prepared 0.5% periodic acid for 5 min followed by a brief wash in distilled water. The sections were then treated in Schiff's reagent for 10 min and developed in several changes of tap water until the water appeared clear. Then the sections were overlaid with filtered Harris' hematoxylin (Luna, 1960) for 30 seconds,

blued in saturated lithium carbonate and rinsed in distilled water. Finally cover slips were mounted with Kaiser's glycerogel (Luna, 1960).

2.4. Statistical Analysis

Statistical analysis was performed using InStat software (version 2.0, GraphPad Software, San Diego, CA). A mean score ± SEM for each group (aged control and AMD) was determined from the scores of all graders for each retinal and choroidal structure. The *p* values were determined by comparing mean scores from the aged control eyes with scores from eyes with AMD using Student *t*-test and assuming unequal variance and two tails. A *p* value <0.05 was considered statistically significant.

3. Results

3.1. Immunolocalization of NOS isoforms in retina

PAS and hematoxylin staining showed the normal morphology of the neural retina in aged control eyes (Fig. 1A), whereas degenerative thin retinas with loss of photoreceptor cells were evident in AMD eyes (Fig. 1B). The endothelial cells of retinal blood vessels in aged control and AMD eyes were intensely labeled for CD34 (Fig. 1C and D). Immunoreactivity for eNOS in aged control retinas was mostly present in the endothelial (EC) and smooth muscle cells (SMC) of retinal arteries and in capillaries. The retinal vasculature had prominent eNOS while neural retina was negative (Fig. 1E), as reported by others (Ju et al., 2001;Meyer et al., 1999). In contrast, immunostaining for nNOS was most prominent in retinal ganglion cells (RGCs) and in neurons of both inner and outer nuclear layers (Fig. 1G). Immunostaining for iNOS was observed in retinal vessels and occasionally in few scattered neurons in the inner nuclear layer (Fig. 1I).

Immunostaining for eNOS and iNOS in AMD retinas was similar in pattern as aged control retina but some AMD cases showed less intense staining (Fig. 1F and J). However, the immunoreactivity for nNOS was significantly lower in RGCs and neurons in AMD eyes (Fig. 1H). Mean immunoreactivity scores for the retinal structures of the aged control and AMD eyes are shown in Figure 2. There was no significant difference in scores for eNOS and iNOS between aged control and AMD retinas. However, immunoreactivity scores for nNOS were significantly lower in RGCs, neurons, and retinal arteries and veins in AMD eyes (p=0.001, p=0.03, p=0.002, and p=0.01, respectively) compared to the aged control retinas (Fig. 2B).

3.2. Immunolocalization of NOS isoforms in choroid

In aged control choroids, PAS and hematoxylin staining showed no deposits or drusen or other pathologic evidence of AMD (Fig. 3A). The choroidal vessels including CC were intensely labeled for CD34 and appeared normal morphologically with broad lumens (Fig. 3C). Compared to aged controls, basal laminar deposits and drusen were often observed in AMD choroids (Fig. 3B). The CC lumens appeared irregular and constricted in AMD eyes (Fig. 3D), and missing in eyes with geographic atrophy.

The immunostaining for eNOS in aged choroid was prominently localized to the CC, to a lesser extent in endothelial cells of large choroidal blood vessels, and individual cells in choroidal stroma (Figs. 3E and 4A). Some cells in suprachoroid, which may be melanocytes or dendritic cells, were also positive for eNOS. Immunoreactivity for nNOS was predominantly present in nuclei of RPE (Fig. 5G, Inset), perivascular nerve fibers that were almost exclusively around the arteries and arterioles (Fig. 5G), smooth muscle cells of arteries and in some scattered cells in stroma (Fig. 3G). Immunostaining for iNOS was localized to choroidal blood vessels and some individual cells in stroma (Fig. 3I). Circulating leukocytes had weak immunostaining for

all three NOS isoforms. There was no staining when primary antibodies were eliminated or non-immune IgG with matched protein concentration as the primary antibody.

In AMD choroids, the immunostaining for all three NOS isoforms appeared weak (Fig. 3F, H and J). Mean immunoreactivity scores for the choroidal structures of the aged control versus AMD eyes are shown in Figure 4. There was significantly less eNOS in choroidal arteries ($p=0.006$) and choroidal cells ($p=0.03$) in AMD eyes than the aged controls (Fig. 4A). The immunoreactivity for nNOS was significantly lower in RPE nuclei, choroidal arteries and veins of AMD subjects ($p=0.001$, $p=0.001$, and $p=0.004$, respectively). In contrast, there was no significant difference in iNOS levels between aged control and AMD choroids (Fig. 4C).

We compared adjacent non-atrophic and atrophic regions of macula in a geographic atrophy (GA) subjects; the pattern and intensity of NOS immunostaining in non-atrophic area was similar to aged control eyes (Fig. 5, left panels). However, in the atrophic area, eNOS was significantly reduced in blood vessels and cells in stroma compared to the non-atrophic area (Fig. 6). iNOS and nNOS were also greatly reduced in perivascular nerve fibers surrounding the arteries (compare Fig. 5G to 5H) and choroidal cells in the atrophic area (Fig. 5, right panels). The immunoreactivity score for eNOS in atrophic area was significantly lower in choroidal arteries ($p=0.0419$) and CC ($p<0.0001$) compared to the non-atrophic areas (Fig. 6). The score for nNOS was significantly lower in perivascular nerve fibers ($p=0.05$) in atrophic area than the non-atrophic area. Whereas the score for iNOS was significantly lower in choroidal veins ($p=0.05$) and CC ($p<0.0001$) in atrophic area than the non-atrophic area (Fig. 6).

In late AMD choroids, we also examined the areas with subretinal choroidal neovascularization (CNV) (Fig. 7) and CNV within disciform scars as well as the choroid underneath the scars and adjacent to CNV (Fig. 8). In subretinal CNV, moderate immunoreactivity for all three NOS isoforms was observed (Fig. 7F, H, J), whereas weak staining was observed not only in choroid underneath the subretinal CNV but in the choroid adjacent to CNV (Fig. 7, left panels). Although there was heterogeneity in the levels of NOS immunoreactivity, the immunoreactivity for eNOS and iNOS was prominent in CNV within disciform scar (Fig. 8C, E), whereas the nNOS was negative in CNV within scar (Fig. 8D). However, in general, the choroid underneath the scar had intense eNOS and nNOS in choroidal cells and perivascular nerve fibers respectively (Fig. 8H and I). The single cells, presumably microglia and resident macrophages, within scar had more intense eNOS and iNOS (Fig. 8H, J).

4. Discussion

Nitric oxide is a potent vasodilator with diverse physiological functions and is a key regulator of ocular blood flow. In this study, we describe the expression pattern of the NOS isoforms (eNOS, nNOS, iNOS) in aged control human eyes. The immunoreactivity levels of eNOS and nNOS were significantly reduced in eyes with AMD. Although NO was not measured directly, these immunohistochemical findings suggest that, in general, there is less NO produced in AMD eyes. The decrease in eNOS and nNOS expressions could be associated with neuronal degeneration in retina and vasoconstriction and hemodynamic changes in AMD choroid.

NO plays an important role in retinal neurotransmission (Sanders and Ward, 1992; Snyder, 1992). In the present study, nNOS immunoreactivity was observed in neurons in the ganglion cell layer and nuclear layers of the retina and the levels were significantly reduced in AMD retina. It has been suggested that amacrine cells might be the most prominent source for NO in the cells located in the RGC layer and INL of the mammalian retina (Kim et al., 2000). These cells may serve as a source of NO to photoreceptors or horizontal cells. Impaired regulation of RGC activities causes photoreceptor degeneration. Death of photoreceptors and subsequent

loss of vision are end points of AMD. We assume that the decrease in retinal nNOS in AMD retinas was probably related to neuronal degeneration.

In the present study, we observed very little retinal iNOS immunoreactivity but some iNOS immunoreactivity was associated with choroidal blood vessels and stroma in aged controls. However, the localization was very similar to eNOS (blood vessels) and nNOS (cells in stroma). The manufacturer actually states in their information sheet that this antibody cross reacts with eNOS and nNOS, which shares 51% amino acid homology with the greatest degree of divergence in the calmodulin binding domain. Therefore, our iNOS localization may represent, at least in part, cross-reactivity of the iNOS antibody with eNOS and nNOS, which would explain why iNOS is present in control subjects retinas and choroids.

In the present study, the two constitutive NOSs (nNOS and eNOS) were significantly reduced in AMD choroid. The submacular human choroid exhibits the highest arteriolar density (Oyster, 1999) to provide sufficient blood flow to the high density of cones located in macula. The dense nitrergic innervation of the choroidal arteries and arterioles, positive for NADPH-diaphorase and nNOS, has been observed in human submacular choroid (Flugel-Koch et al., 1994; Flügel et al., 1994) and other species (Bergua et al., 1996; Yamamoto et al., 1993). The presence of nNOS/NADPH-diaphorase positive neurons and the high density of nerve fibers could be responsible for regulating submacular arteriolar blood flow in choroid (Trivino et al., 2002). These nerve fibers also mediate vasodilation in choroid. Mann et al. (Mann et al., 1995) have shown a similar vasodilative role of NO in the regulation of choroidal blood flow in cat eyes. Kiel (Kiel, 1999) showed the influence of NOS inhibition on lowering autoregulatory limit in rabbits and hypothesized that both neuronal and endothelial NO play a role in choroidal regulatory mechanisms. It is now well established that the choroidal vasculature plays a pivotal role in development of AMD. Friedman proposed a hemodynamic model for AMD that suggests AMD is a vascular disorder characterized by impairment of choroidal perfusion (Friedman, 1997). In addition, the average blood flow measured in the submacular choroid in AMD patients has been shown to be reduced up to 37% compared to aged control subjects (Grunwald et al., 1998a; Grunwald et al., 1998b). A significant age-related reduction in the vasoactive intestinal peptide (VIP) positive vasodilatory nerve fibers in submacular choroid has also been reported (Jablonski et al., 2007). We have previously observed severe choriocapillaris constriction in postmortem eyes with geographic atrophy (McLeod et al., 2002). Taken together, a decrease in nNOS and eNOS in AMD choroid could contribute to the decline in the neural and endothelial control of choroidal blood flow in the submacular region resulting in microcirculatory changes in AMD choroid.

One interesting finding of this study is expression of nNOS in RPE nuclei. Originally nNOS was discovered in neurons, but later was also found in glial cells (Kugler and Drenckhahn, 1996; Tolias et al., 1999). It was mainly distributed in the cytoplasm (Kugler and Drenckhahn, 1996; Riefler and Firestein, 2001). The presence of nNOS in nucleus has been reported more recently in cultured neonatal cardiomyocytes (Xu et al., 1999), pancreatic β-cells (Lajoix et al., 2001), brown adipocytes (Giordano et al., 2002), mast cells (Gilchrist et al., 2004) and rat astrocytes (Yuan et al., 2004). The presence of NO in the subcellular compartments can be of significance in modulating diverse targets. Yuan et al. suggested that nuclear nNOS might represent a role for nNOS in transcriptional regulation (Yuan et al., 2004). One study described subcellular distribution of NOS and caveolin-1, a prominent NOS-interacting protein, in rat polymorphonuclear neutrophils (PMNs) (Saini et al., 2006). Their results provided evidence of active nNOS and iNOS in the subcellular compartments including nucleus and suggested that NOS interaction with caveolin-1 in rat PMNs may serve a definitive role in the compartmentalized redox signaling. It has become increasingly evident that the redox status of RPE cells plays a critical role in combating oxidant stress (Cai et al., 2000). Ample evidence in the literature suggests that oxidative stress may be a contributing factor to RPE dysfunction

in AMD (Beatty et al., 2000). Therefore, it is possible that the reduction of nNOS in RPE nuclei in AMD choroid could possibly alter the redox status of RPE in AMD.

In late AMD eyes, subretinal CNV and CNV within disciform scars had prominent localization of eNOS and iNOS, whereas weak staining was observed not only in choroid underneath the subretinal CNV but also in the choroid adjacent to CNV. The disciform scar is usually vascularized, almost invariably from the choroidal circulation but sometimes with retinal contributions as well, and can have both subretinal and sub-RPE components (Green, 1999). However, the CNV in scars is usually regressing or at least stabilized and not expanding. None of CNV formations in our AMD cohort were in growth stage; all were present within disciform scars, and were likely quiescent. Tissue hypoxia is the common denominator and the major trigger of local angiogenesis stimulators and proteolytic enzymes are a prerequisite for neovascularization (Hanahan and Folkman, 1996; Steen et al., 1998), which together cooperatively participate in the progressive growth of CNV membranes in AMD. Hypoxia is one of the most potent inducers of the vascular endothelial growth factor (VEGF) expression, a major regulator of the CNV among the angiogenic factors studied (Kim, 2007). NO mediates the proangiogenic response of several key factors including VEGF (Papapetropoulos et al., 1997) and the VEGF-mediated angiogenesis requires NO production from activated eNOS. Recently, McLaren et al. has demonstrated that hypoxia-induced molecules, including NOS and VEGF, were upregulated within cerebral cortex of acutely anemic rats (McLaren et al., 2007). Previous reports have shown that eNOS and its regulation via phosphorylation/dephosphorylation events as a key modulator in angiogenesis (Bernatchez et al., 2005; Duda et al., 2004). In this study, Figure 8 demonstrates elevated NOS associated with CNV. These findings support the notion that NOS could act positively on the VEGF promoter activity under hypoxia depending upon the concentration, environmental oxygen tension and cell type.

In summary, nNOS immunoreactivity was localized in cells in RGC and nuclear layers of the retina, RPE nuclei, perivascular nerve fibers, and blood vessels in choroid. Immunoreactivity for eNOS and iNOS was confined almost exclusively to the retinal and choroidal blood vessels. Some stromal melanocytes and/or dendritic cells in choroid were also positive for eNOS. In AMD eyes, the immunoreactivity for the constitutive NOS's (nNOS and eNOS) was significantly lower in retina and choroid. The reduced levels of nNOS and eNOS in choroid were probably related to the loss of CC and reduction of perivascular nerve fibers in AMD. The decrease in nNOS and eNOS expression in choroid could be associated with vasoconstriction and hemodynamic changes in AMD. These findings lend support to the possibility that reduced NO may play critical role in reducing blood volume to submacular choroid which is critical for central visual function.

Acknowledgments

This work was supported by NIH grants: EY-01765 (Wilmer) and R01-EY016151 (GL), Research to Prevent Blindness (Wilmer), the Foundation Fighting Blindness (GL), and Altsheler Durell Foundation. Gerard Lutty received an RPB senior scientific investigator award. The authors are grateful to the eye donors and their relatives for their generosity and also to Janet Sunness, MD, and Carol Applegate at the Great Baltimore Medical Center (Baltimore, MD) for helping us acquire eyes from subjects with AMD.

Supported by: NIH Grants R01-EY016151 (GL), EY-01765 (Wilmer); unrestricted funds from Research to Prevent Blindness (Wilmer); Foundation Fighting Blindness (GL); and the Altsheler-Durell Foundation. G. Lutty received an RPB senior investigator award in 2008.

References

Alderton WK, Cooper CE, Knowles RG. Nitric oxide synthases: structure, function and inhibition. Biochem J 2001;357:593–615. [PubMed: 11463332]

Beatty S, Koh H, Phil M, Henson D, Boulton M. The role of oxidative stress in the pathogenesis of age-related macular degeneration. Surv Ophthalmol 2000;45:115–134. [PubMed: 11033038]

Bergua A, Mayer B, Neuhuber WL. Nitrergic and VIPergic neurons in the choroid and ciliary ganglion of the duck Anis carina. Anat Embryol (Berl) 1996;193:239–248. [PubMed: 8881473]

Bernatchez PN, Bauer PM, Yu J, Prendergast JS, He P, Sessa WC. Dissecting the molecular control of endothelial NO synthase by caveolin-1 using cell-permeable peptides. Proc Natl Acad Sci U S A 2005;102:761–766. [PubMed: 15637154]

Bhutto IA, Kim SY, McLeod D, S, Merges CA, Fukai N, Olsen BR, Lutty GA. Localization of collagen XVIII and the endostatin portion of collagen XVIII in aged human control eyes and eyes with age-related macular degeneration. Invest. Ophthalmol. Vis. Sci 2004;45:1544–1552. [PubMed: 15111613]

Boulanger CM, Heymes C, Benessiano J, Geske RS, Levy BI, Vanhoutte PM. Neuronal nitric oxide synthase is expressed in rat vascular smooth muscle cells: activation by angiotensin II in hypertension. Circ Res 1998;83:1271–1278. [PubMed: 9851944]

Cai J, Nelson KC, Wu M, Sternberg P Jr. Jones DP. Oxidative damage and protection of the RPE. Prog Retin Eye Res 2000;19:205–221. [PubMed: 10674708]

Cioffi, GA.; Granstam, E. Ocular circulation. Vol. 10 ed.. Mosby; St. Louis: 2002.

Duda DG, Fukumura D, Jain RK. Role of eNOS in neovascularization: NO for endothelial progenitor cells. Trends Mol Med 2004;10:143–145. [PubMed: 15162796]

Flugel-Koch C, Kaufman P, Lutjen-Drecoll E. Association of a choroidal ganglion cell plexus with the fovea centralis. Invest Ophthalmol Vis Sci 1994;35:4268–4272. [PubMed: 7528181]

Flügel C, Tamm ER, Mayer B, Lütjen-Drecoll E. Species differences in choroidal vasodilative innervation: Evidence for specific intrinsic nitrergic and VIP-positive neurons in the human eye. Invest. Ophthalmol. Vis. Sci 1994;35:592–599. [PubMed: 7509326]

Friedman E. A hemodynamic model of the pathogenesis of age-related macular degeneration. Am J Ophthalmol 1997;124:677–682. [PubMed: 9372722]

Geyer O, Podos SM, Mittag T. Nitric oxide synthase activity in tissues of the bovine eye. Graefes Arch Clin Exp Ophthalmol 1997;235:786–793. [PubMed: 9439972]

Gilchrist M, McCauley SD, Befus AD. Expression, localization, and regulation of NOS in human mast cell lines: effects on leukotriene production. Blood 2004;104:462–469. [PubMed: 15044250]

Giordano A, Tonello C, Bulbarelli A, Cozzi V, Cinti S, Carruba MO, Nisoli E. Evidence for a functional nitric oxide synthase system in brown adipocyte nucleus. FEBS Lett 2002;514:135–140. [PubMed: 11943139]

Green WR. Histopathology of age-related macular degeneration. Mol Vis 1999;5:27. [PubMed: 10562651]

Griffith OW, Stuehr DJ. Nitric oxide synthases: properties and catalytic mechanism. Annu Rev Physiol 1995;57:707–736. [PubMed: 7539994]

Grunwald J, Hariprasad S, DuPont J. Effect of aging on foveolar choroidal circulation. Arch. Ophthalmol 1998a;116:150–154. [PubMed: 9488265]

Grunwald J, Hariprasad S, DuPont J, Maguire M, Fine S, Brucker A, Maguire A, Ho A. Foveolar choroidal blood flow in age-related macular degeneration. Invest. Ophthalmol. Vis. Sci 1998b;39:385–390. [PubMed: 9477998]

Hanahan D, Folkman J. Patterns and emerging mechanisms of the angiogenic switch during tumor genesis. Cell 1996;86:353–364. [PubMed: 8756718]

Ichihara A, Inscho EW, Imig JD, Navar LG. Neuronal nitric oxide synthase modulates rat renal microvascular function. Am J Physiol 1998;274:F516–524. [PubMed: 9530268]

Jablonski MM, Iannaccone A, Reynolds DH, Gallaher P, Allen S, Wang X, Reiner A. Age-related decline in VIP-positive parasympathetic nerve fibers in the human submacular choroid. Invest Ophthalmol Vis Sci 2007;48:479–485. [PubMed: 17251439]

Ju WK, Gwon JS, Kim KY, Oh SJ, Kim SY, Chun MH. Up-regulated eNOS protects blood-retinal barrier in the L-arginine treated ischemic rat retina. Neuroreport 2001;12:2405–2409. [PubMed: 11496119]

Kashiwagi S, Kajimura M, Yoshimura Y, Suematsu M. Nonendothelial source of nitric oxide in arterioles but not in venules: alternative source revealed in vivo by diaminofluorescein microfluorography. Circ Res 2002;91:e55–64. [PubMed: 12480826]

Kiel JW. Modulation of choroidal autoregulation in the rabbit. Exp Eye Res 1999;69:413–429. [PubMed: 10504275]

Kim IB, Oh SJ, Chun MH. Neuronal nitric oxide synthase immunoreactive neurons in the mammalian retina. Microsc Res Tech 2000;50:112–123. [PubMed: 10891875]

Kim R. Introduction, mechanism of action and rationale for anti-vascular endothelial growth factor drugs in age-related macular degeneration. Indian J Ophthalmol 2007;55:413–415. [PubMed: 17951895]

Kugler P, Drenckhahn D. Astrocytes and Bergmann glia as an important site of nitric oxide synthase I. Glia 1996;16:165–173. [PubMed: 8929903]

Lajoix AD, Reggio H, Chardes T, Peraldi-Roux S, Tribillac F, Roye M, Dietz S, Broca C, Manteghetti M, Ribes G, Wollheim CB, Gross R. A neuronal isoform of nitric oxide synthase expressed in pancreatic beta-cells controls insulin secretion. Diabetes 2001;50:1311–1323. [PubMed: 11375331]

Luna, LG. Manual of Histologic Staining Methods of the Armed Forces Institute of Pathology. McGraw-Hill Book Co.; New York, NY: 1960.

Lutjen-Drecoll E. Choroidal innervation in primate eyes. Exp Eye Res 2006;82:357–361. [PubMed: 16289045]

Lutty GA, Merges C, Threlkeld AB, Crone S, McLeod DS. Heterogeneity in localization of isoforms of TGF-b in human retina, vitreous, and choroid. Invest. Ophthalmol. Vis. Sci 1993;34:477–487. [PubMed: 7680639]

Mann RM, Riva CE, Stone RA, Barnes GE, Cranstoun SD. Nitric oxide and choroidal blood flow regulation. Invest Ophthalmol Vis Sci 1995;36:925–930. [PubMed: 7706041]

McLaren AT, Marsden PA, Mazer CD, Baker AJ, Stewart DJ, Tsui AK, Li X, Yucel Y, Robb M, Boyd SR, Liu E, Yu J, Hare GM. Increased expression of HIF-1alpha, nNOS, and VEGF in the cerebral cortex of anemic rats. Am J Physiol Regul Integr Comp Physiol 2007;292:R403–414. [PubMed: 16973934]

McLeod DS, Grebe R, Bhutto I, Merges C, Baba T, Lutty GA. Relationship between RPE and choriocapillaris in age-related macular degeneration. Invest Ophthalmol Vis Sci. Apr 8;2009 [Epub ahead of print]

McLeod DS, Lefer DJ, Merges C, Lutty GA. Enhanced expression of intracellular adhesion molecule-1 and P-selectin in the diabetic human retina and choroid. Am. J. Pathol 1995;147:642–653. [PubMed: 7545873]

McLeod DS, Taomoto M, Otsuji T, Green WR, Sunness JS, Lutty GA. Quantifying changes in RPE and choriocapillaris in eyes with age-related macular degeneration. Invest. Ophthalmol. Vis. Sci 2002;43:1986–1993. [PubMed: 12037009]

Meyer P, Champion C, Schlotzer-Schrehardt U, Flammer J, Haefliger IO. Localization of nitric oxide synthase isoforms in porcine ocular tissues. Curr Eye Res 1999;18:375–380. [PubMed: 10373000]

Moncada S, Palmer RM, Higgs EA. Nitric oxide: physiology, pathophysiology, and pharmacology. Pharmacol Rev 1991;43:109–142. [PubMed: 1852778]

Nozaki K, Moskowitz MA, Maynard KI, Koketsu N, Dawson TM, Bredt DS, Snyder SH. Possible origins and distribution of immunoreactive nitric oxide synthase-containing nerve fibers in cerebral arteries. J Cereb Blood Flow Metab 1993;13:70–79. [PubMed: 7678014]

Oyster, CW. The human eye. Structure and function. Sinauer Associates; Sunderland, Massachussetts: 1999.

Page C, Rose M, Yacoub M, Pigott R. Antigenic heterogeneity of vascular endothelium. Am. J. Pathol 1992;141:673–683. [PubMed: 1519671]

Palmer RM, Ferrige AG, Moncada S. Nitric oxide release accounts for the biological activity of endothelium-derived relaxing factor. Nature 1987;327:524–526. [PubMed: 3495737]

Papapetropoulos A, Garcia-Cardena G, Madri JA, Sessa WC. Nitric oxide production contributes to the angiogenic properties of vascular endothelial growth factor in human endothelial cells. J Clin Invest 1997;100:3131–3139. [PubMed: 9399960]

Riefler GM, Firestein BL. Binding of neuronal nitric-oxide synthase (nNOS) to carboxyl-terminal-binding protein (CtBP) changes the localization of CtBP from the nucleus to the cytosol: a novel function for targeting by the PDZ domain of nNOS. J Biol Chem 2001;276:48262–48268. [PubMed: 11590170]

Ruskell GL. Facial parasympathetic innervation of the choroidal blood vessels in monkeys. Exp Eye Res 1971;12:166–172. [PubMed: 5000886]

Saini R, Patel S, Saluja R, Sahasrabuddhe AA, Singh MP, Habib S, Bajpai VK, Dikshit M. Nitric oxide synthase localization in the rat neutrophils: immunocytochemical, molecular, and biochemical studies. J Leukoc Biol 2006;79:519–528. [PubMed: 16387842]

Sanders KM, Ward SM. Nitric oxide as a mediator of nonadrenergic noncholinergic neurotransmission. Am J Physiol 1992;262:G379–392. [PubMed: 1347974]

Snyder SH. Nitric oxide and neurons. Curr Opin Neurobiol 1992;2:323–327. [PubMed: 1353698]

Steen B, Sejersen S, Berglin L, Seregard S, Kvanta A. Matrix metalloproteinases and metalloproteinase inhibitors in choroidal neovascular membranes. Invest Ophthalmol Vis Sci 1998;39:2194–2200. [PubMed: 9761302]

Toda N, Okamura T. The pharmacology of nitrxic oxide in the peripheral nervous system of blood vessels. Pharmacol Rev 2003;55:271–324. [PubMed: 12773630]

Tolias CM, McNeil CJ, Kazlauskaite J, Hillhouse EW. Superoxide generation from constitutive nitric oxide synthase in astrocytes in vitro regulates extracellular nitric oxide availability. Free Radic Biol Med 1999;26:99–106. [PubMed: 9890645]

Trivino A, De Hoz R, Salazar JJ, Ramirez AI, Rojas B, Ramirez JM. Distribution and organization of the nerve fiber and ganglion cells of the human choroid. Anat Embryol (Berl) 2002;205:417–430. [PubMed: 12382145]

Xu KY, Huso DL, Dawson TM, Bredt DS, Becker LC. Nitric oxide synthase in cardiac sarcoplasmic reticulum. Proc Natl Acad Sci U S A 1999;96:657–662. [PubMed: 9892689]

Yamamoto R, Bredt DS, Snyder SH, Stone RA. The localization of nitric oxide synthase in the rat eye and related cranial ganglia. Neuroscience 1993;54:189–200. [PubMed: 7685860]

Yuan Z, Liu B, Yuan L, Zhang Y, Dong X, Lu J. Evidence of nuclear localization of neuronal nitric oxide synthase in cultured astrocytes of rats. Life Sci 2004;74:3199–3209. [PubMed: 15094321]

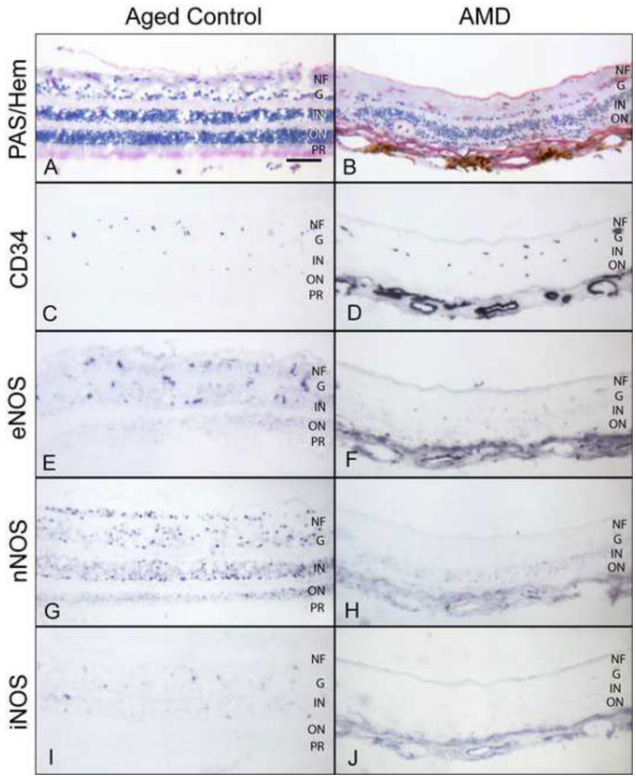

Figure 1.

Immunoreactivity for NOS isoforms in the aged control (subject 10) and AMD (subject 18) retina. PAS and hematoxylin staining shows normal morphological features of the aged control (A) and a degenerative thin retina with loss of photoreceptors in AMD (B). Retinal blood vessels are labeled with CD34 (C, D). Note the AMD retina is thin so choroidal blood vessels are present in the pictures and stain with CD34 (D). In aged control retina, eNOS antibody staining is present in the retinal blood vessels and in a few scattered cells in ganglion cell and inner nuclear layer, which may be retinal capillaries (E). nNOS is prominent in ganglion cells and neurons in both inner and outer nuclear layers (G). iNOS is present in a few scattered cells in the inner nuclear layer (I). In this AMD retina, immunoreactivity for NOS isoforms is significantly weaker than in the control retina (F–J). Magnification bar (A–J) = 100 μm. (NF=nerve fiber layer; G=ganglion cell layer; IN=Inner nuclear; ON=outer nuclear; PR=photoreceptors)

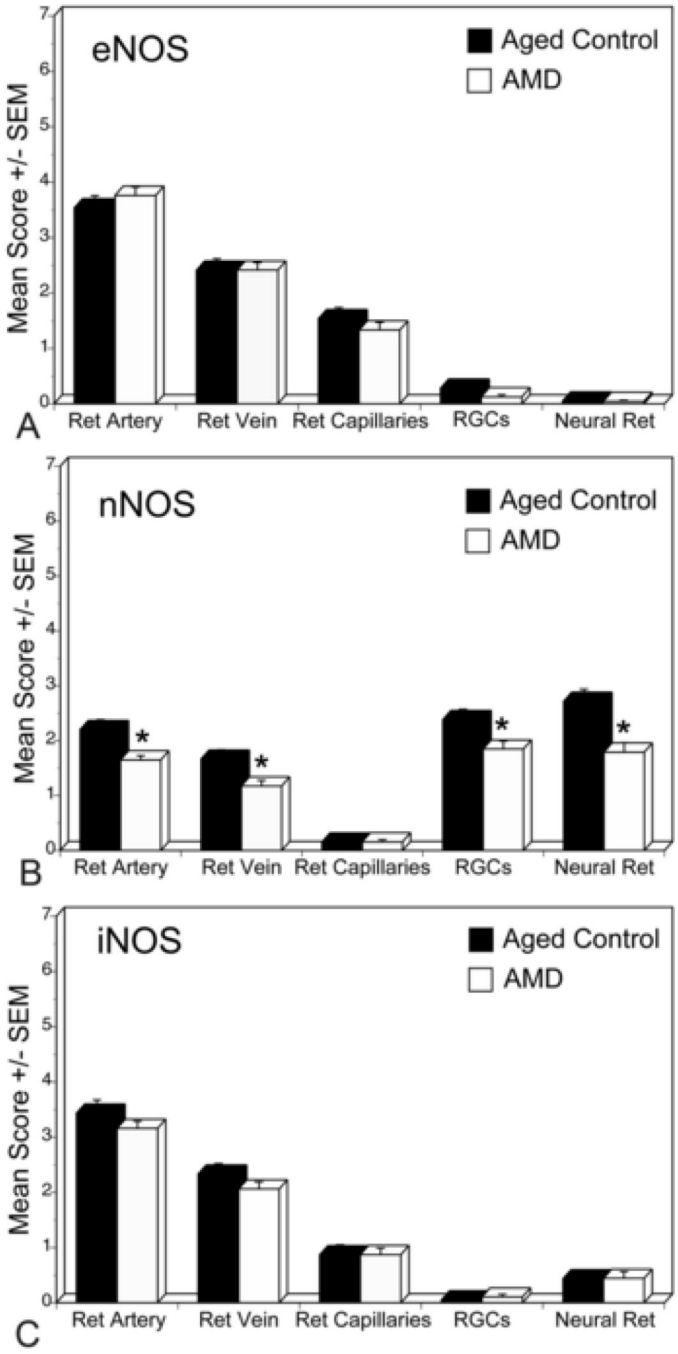

Figure 2.

Mean immunoreactivity scores±SEM for NOS isoforms in retinal structures of all aged control (black) and AMD (white) eyes. The immunoreactivity scores for nNOS (B) were significantly lower in RGCs, neural cells, and retinal arteries and veins in AMD retina compared to aged control. There were no significant difference in eNOS (A) and iNOS (C) immunoreactivity levels for retinal structures between aged and AMD retinas. The significance of the difference between the groups by t test is indicated: *= $p<0.05$.

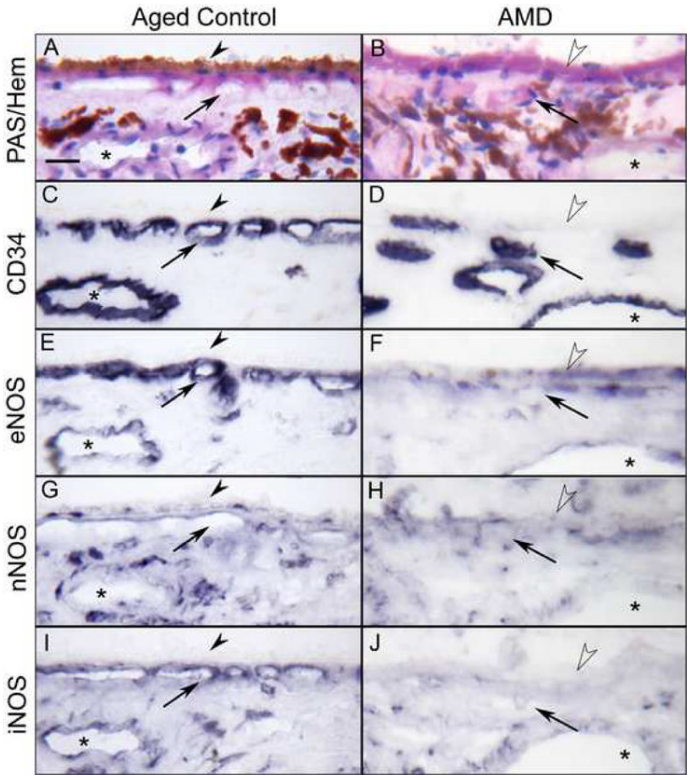

Figure 3.

Immunoreactivity for NOS isoforms in aged control (subject 2) and AMD (subject 13) choroid. PAS and hematoxylin staining show morphological features of choroids (A, B). Note that thickened PAS positive Bruch's membrane (open arrowheads) in AMD choroid (B). In aged control choroid, large and medium choroidal vessels (asterisk) and choriocapillaris (CC; arrows) are intensely labeled for CD34 and appear morphologically normal with broad lumens (C), whereas there is loss of CC and CC lumens appear constricted in AMD choroid (D). In aged control choroid, eNOS is prominently localized to the CC and, to a lesser extent, in endothelial cells of medium sized choroidal blood vessels and a few individual cells in choroidal stroma (E). nNOS is present in RPE nuclei, and perivascular nerve fibers and cells in stroma (G). iNOS is localized to endothelial cells of blood vessels and individual cells in stroma (I). In AMD choroid, immunoreactivity for NOS isoforms is greatly reduced compared to the control subject (F, H, J). Magnification bar (A–J) = 20 μm.

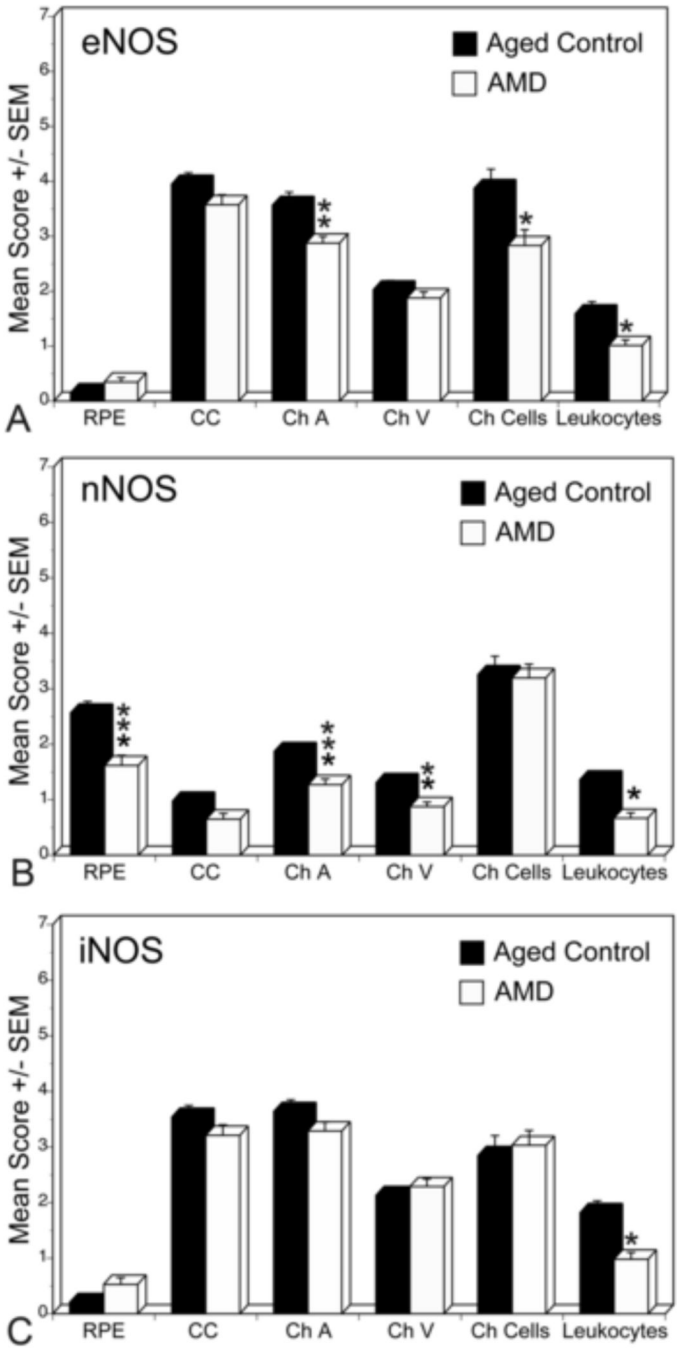

Figure 4.

Mean immunoreactivity scores±SEM for NOS isoforms in choroidal structures of aged control (black) and AMD (white) eyes. The immunoreactivity scores for eNOS were significantly lower in choroidal arteries, cells in stroma, and leukocytes in blood vessel lumens in AMD choroid. nNOS was significantly lower in RPE nuclei, arteries and veins as well as leukocytes. There was no significant difference in iNOS levels between aged control and AMD choroids except in leukocytes. The significance of the difference between the groups by t test is indicated: *= $p<0.01$, **= $p<0.005$, ***= $p<0.001$.

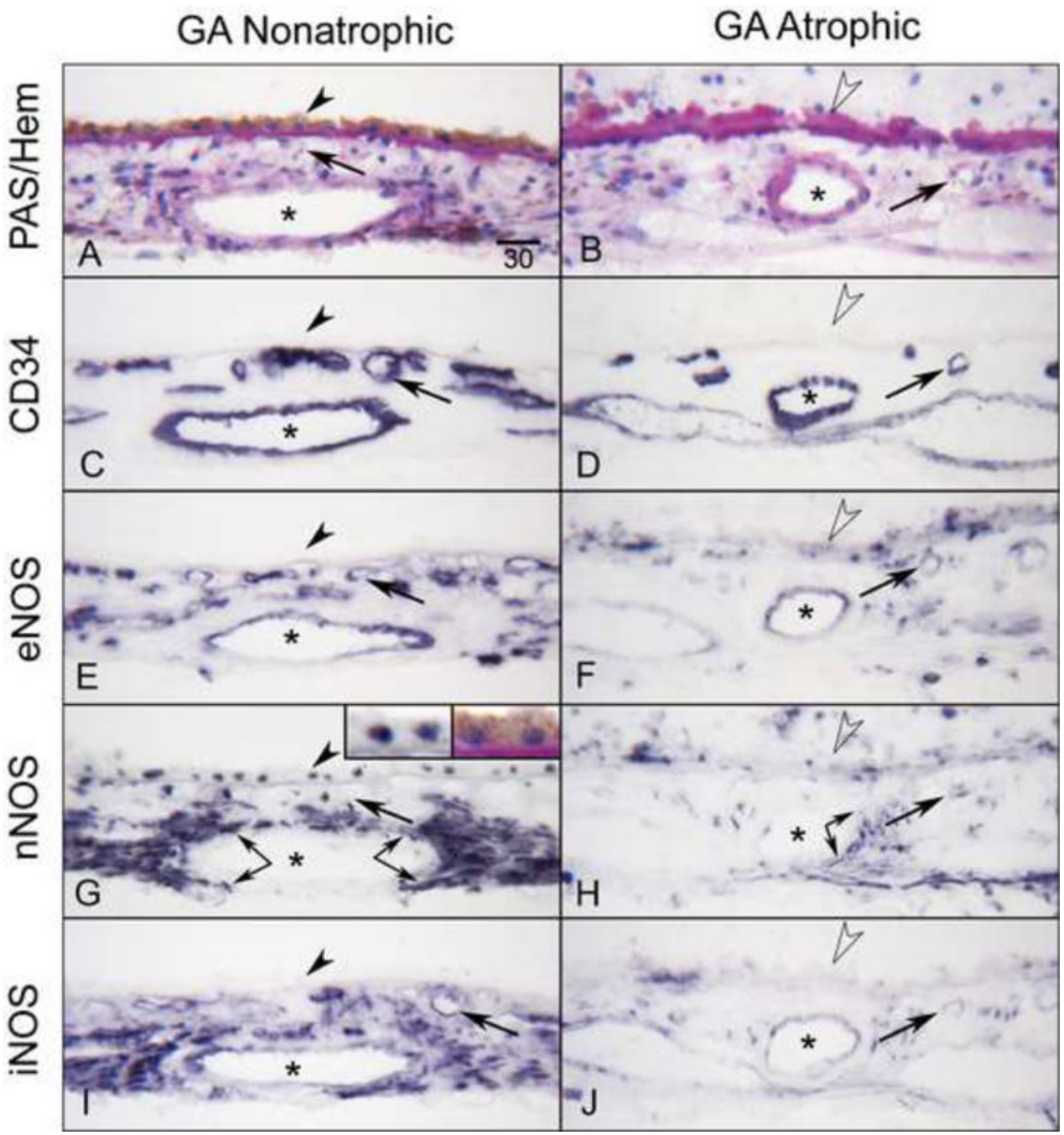

Figure 5.

Immunoreactivity for NOS isoforms in AMD eye with geographic atrophy (subject 15). Note that the non-atrophic area (A) of choroid has RPE (arrowhead) and there is PAS-positive thickened Bruch's membrane (open arrowhead) but there is no RPE in atrophic area (B). CD34 demonstrates CC (arrows) is limited in the atrophic area compared to the non-atrophic area (C, D). In non-atrophic area, eNOS (E) is prominent in CC and endothelial cells of large blood vessels (asterisks) as well as cells in stroma, which may include melanocytes. nNOS (G) is prominent in RPE nuclei (at high magnification, Inset) and perivascular nerve fibers (double arrows). iNOS (I) appears similar to nNOS. The similarity with nNOS may be due to cross

reactivity of the antibodies. Immunoreactivity for NOS isoforms is greatly reduced in choroid structures in the atrophic area (F, H, J). Magnification bar (A–J) = 30 μm.

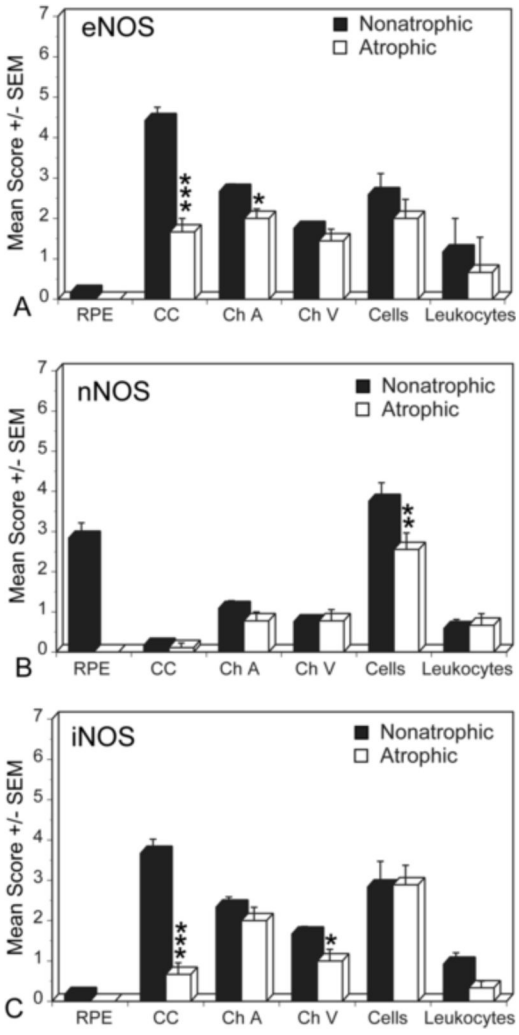

Figure 6.

Mean immunoreactivity scores±SEM for NOS isoforms in choroidal structures comparing atrophic (black) and non-atrophic (white) areas in a geographic atrophy (GA) subjects. The immunoreactivity scores for eNOS were significantly lower in choroidal arteries and CC in atrophic area compared to the non-atrophic area. The mean score for nNOS was significantly lower in perivascular nerve fibers, whereas the score for iNOS was significantly lower in choroidal veins and CC in atrophic area than in the non-atrophic area. The significance of the difference between the groups by t test is indicated: *= $p<0.01$, **= $p<0.005$, ***= $p<0.001$.

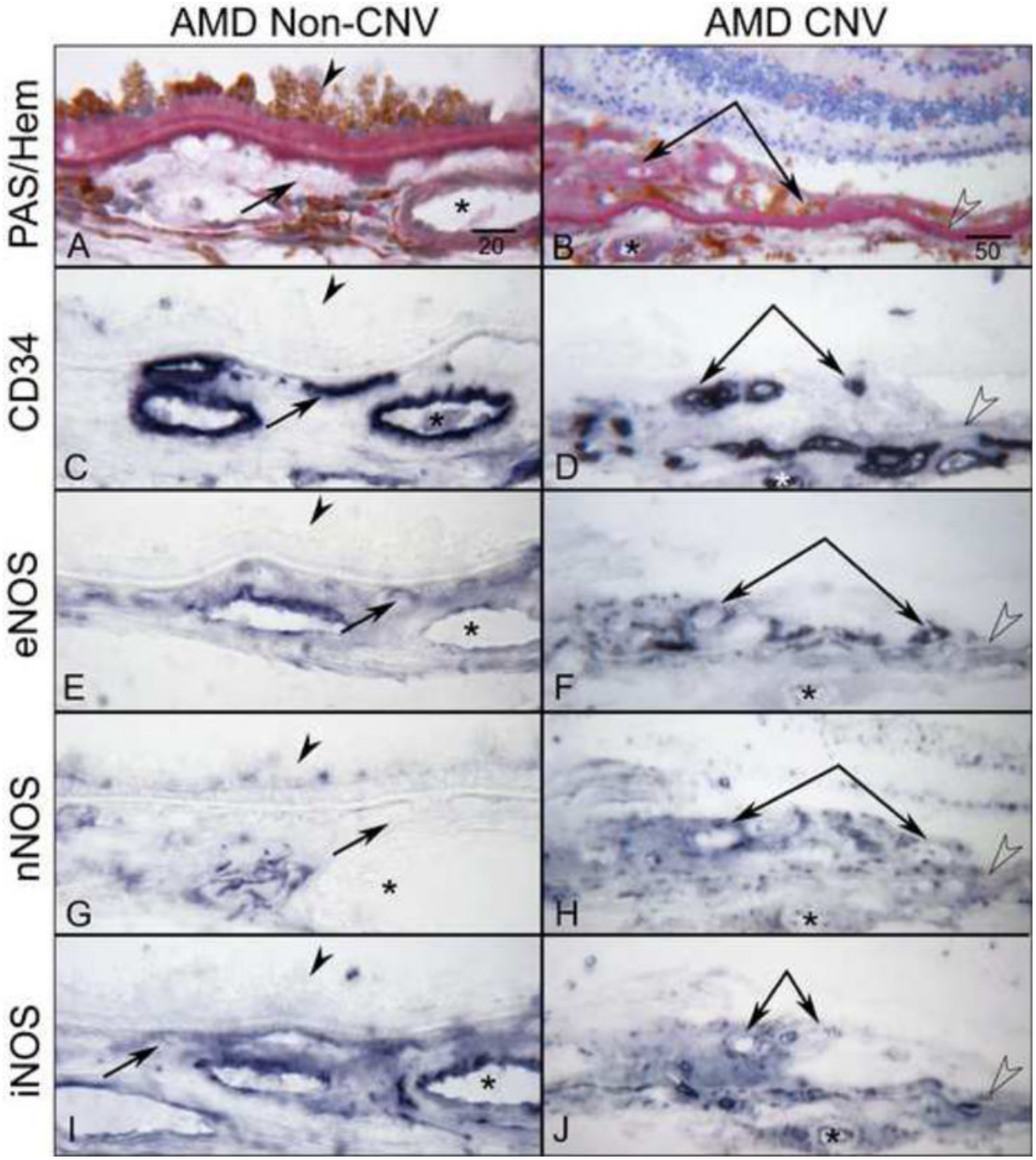

Figure 7.

Immunoreactivity for NOS isoforms in subretinal CNV and choroid under and adjacent to CNV (non-CNV) areas in late AMD eye (subject 19). PAS and hematoxylin staining demonstrates basal laminar deposits under hypertrophic RPE (arrowhead) in choroid with no CNV (A) and subretinal CNV (double arrows) with PAS-positive Bruch's membrane (open arrowhead) (B). The CC (arrows), choroidal vessels (asterisks) and subretinal CNV (double arrows) are intensely positive for CD34 (C, D). Note the moderate immunoreactivity for all three NOS isoforms is seen in subretinal CNV (F, H, J), whereas weak staining for nNOS is observed not only in choroid underneath the subretinal CNV but in the choroid adjacent to CNV (G, H).

Moderate eNOS and iNOS staining are observed in choroid with no CNV (E, I). Magnification bar in left panels = 20 μm and in right panels = 50 μm.

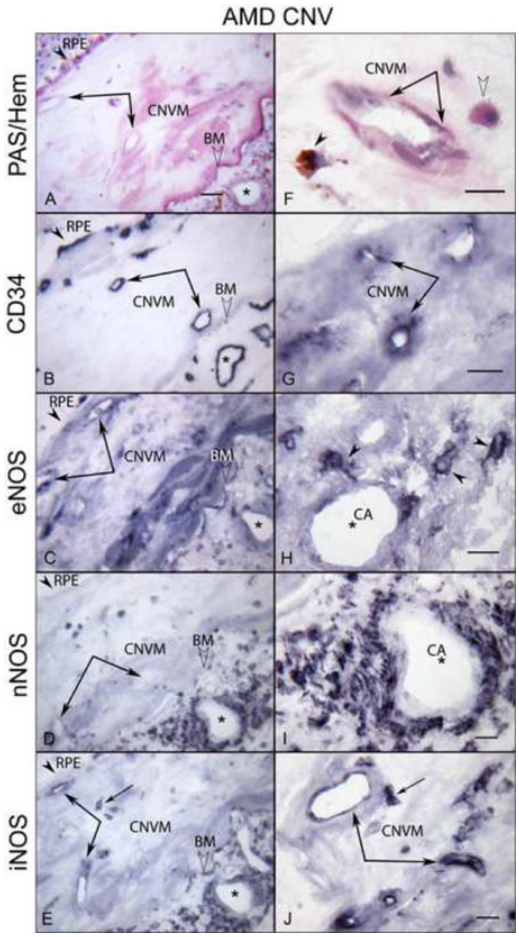

Figure 8.

Immunoreactivity for NOS isoforms in CNV within disciform scar and the choroid underneath the scar in late AMD eye (subject 20). In left panels, (A) PAS and hematoxylin staining demonstrates CNV within scar (double arrows) and PAS-positive Bruch's membrane (BM; open arrowhead) and choroidal vessels (asterisks) underneath the scar. RPE are indicated by arrowhead. (B) The CNV and choroidal vessels are positive for CD34. Immunoreactivity for eNOS (C) and iNOS (E) is prominent in CNV, whereas the nNOS is negative in CNV (D). Note that the choroidal cells and perivascular nerve fibers of choroid underneath the scar exhibit intense immunoreactivity for NOS isoforms (C, D, E). In right panels (at higher magnification), PAS-positive pigmented cells (arrowhead) and apparent monocytes (open arrowhead) are seen close to CNV (double arrows) (F). The CNV is positive for CD34 (G). The intense eNOS immunoreactivity in single cells presumably monocytes in choroid underneath the scar (H), whereas nNOS is present in perivascular nerve fibers (I). (J) iNOS is in CNV and presumably monocytes (arrow). Magnification bar in left panels = 50 μm and right panels = 20 μm.

Table 1

Characteristics of human subjects

Subject	Time (hours)		Age/race/sex	Primary cause of death	Medical history	Ocular diagnosis
	DET	PMT				
Aged						
1	6	29	70/C/M	Myocardial infarction/Obesity	HTN	Normal
2	3.5	29	73/C/F	Colon cancer		Normal
3	2.5	33	75/C/F	Heart disease		Normal
4	3	24	75/C/M	Bronchitis (Lung cancer)	Smoker	Normal
5	7	27	76/C/F	Lung cancer	HTN	Normal
6	1	26	77/C/M	COPD	HTN	Normal
7	2.5	28	80/C/M	COPD		Normal
8	7.15	28	80/C/M	Intracranial hemorrhage	HTN, angioplasty	Normal
9	3	15	82/C/M	Metastasis Brain cancer		Normal
10	3	16	83/C/M	Cardiac respiratory arrest		Normal
11	4	31	84/C/M	Cardiac arrhythmia		Normal (IOL; OU)
12	5	26	86/C/F	Respiratory failure	COPD	Normal
13	3	32	86/C/M	CVA	HTN, COPD	Normal
AMD						
1	3.5	34	61/C/M	Metastasis esophageal CA		AMD, early
2	4	33	74/C/M	Prostate cancer		AMD, early
3	2	38	76/C/F	Brain Death		AMD, early
4	1.5	33	77/C/M	CVA (Sepsis)		AMD, early
5	4	28	77/C/F	GI Bleed	Smoker	AMD, early
6	6	26	79/C/F	Lymphoma		AMD, early
7	3	33	79/C/M	Pneumonia	HTN, Prostate CA	AMD, early
8	5	29	81/C/F	Myocardial infarction	HTN	AMD, early
9	7	28	82/C/M	Pneumonia		AMD, early
10	3	12	83/C/M	Prostate cancer	DM, HTN	AMD, early
11	1.5	21	95/C/F	Pneumonia		AMD, early
12	2	33	98/C/F	Old age		AMD, early
13	5	26	78/C/F	CAD	DM, HTN	AMD (GA), late
14	7.5	26	79/C/M	COPD		AMD (GA), late
15	6	9	88/C/M	CHF, CAD	Smoker	AMD (GA), late
16	3	36	94/C/M	Cardiac failure		AMD (disciform scar, GA), late
17	3.5	?	95/C/M	Cardiomyopathy		AMD (disciform scar, GA), late
18	4.5–5	11	105/C/M	COPD		AMD (disciform scar, GA), late
19	7	30	75/C/M	Aspiration pneumonia		AMD (scar w/CNV), late
20	4	17	80/C/F	Colon cancer	End-stage colon CA	AMD (scar w/CNV), late
21	7	28	89/C/F	Pancreatic cancer		AMD (scar w/CNV), late
22	4	20	93/C/F	Multi system failure	DM, HTN	AMD (scar w/CNV), late

DET, death to enucleation time; PMT, postmortem time (death to fixation); C, Caucasian; AMD, age-related macular degeneration; CVA, cardiovascular arrest; DM, diabetes mellitus; HTN, hypertension; COPD, chronic obstructive pulmonary disease; GA, geographic atrophy; CA, cancer